Proceedings of the 2012 IFAC Workshop on Automatic Control in Offshore Oil and Gas Production, Norwegian University of Science and Technology, Trondheim, Norway, May 31 - June 1, 2012

RoboGas^{Inspector} – A Mobile Robotic System for Remote Leak Sensing and Localization in Large Industrial Environments: Overview and First Results

Samuel Soldan. Gero Bonow. Andreas Kroll

University of Kassel, Faculty of Mechanical Engineering, Department of Measurement and Control, Mönchebergstraße 7, 34125 Kassel, Germany (e-mail: {samuel.soldan, gero.bonow, andreas.kroll}@mrt.uni-kassel.de)

Abstract: In order to automate the routine inspections in large industrial environments a mobile robotic system is being developed in the project RoboGas^{Inspector}. The robot's sensor-head consists of different instruments for remote sensing using multiple measurement principles. First results show that passive IR-thermographic imaging can be used to detect leaks in pipes as well as liquid spills on the ground. The measurable effects are the temperature profile disturbance due to expansion of pressured gas and evaporative cooling, respectively. Tunable Diode Laser Absorption Spectroscopy (TDLAS) measurement systems provide for quantitative gas concentration measurements and feature a high sensitivity due to the active measurement principle. On the contrary, TDLAS systems measure just the concentration along a path at a time and require a diffusely reflecting background. Using a Pan-Tilt Unit, objects/areas can be scanned and abnormal gas concentrations can be identified. This contribution introduces the project RoboGas^{Inspector} and presents the used measurement technology as well as first results.

Keywords: Service robotics, industrial inspection, remote leak detection, TDLAS, thermography.

1. INTRODUCTION

Within the oil and gas industry, remote operation of offshore production facilities is of key interest due to the extremely demanding environments. Of particular importance is tail-end production due to the technically and commercially difficult situation (Vatland et al. 2007). During normal operation, many platforms are already remotely operated, while specialized tasks such as inspection and maintenance still require humans on site (Skourup and Pretlove 2011). This has driven research in mobile robotics to enable remote operation of such tasks. Proposed approaches include ground-based autonomous mobile robots for inspection (Graf and Pfeiffer 2008) and portal robots for inspection and intervention (Skourup and Pretlove 2011).

Aforementioned work addresses majorly mobility and accessibility problems. This contribution addresses the problem of detecting and localizing fluid leakages in plants and industrial infrastructure using mobile robots. The detection of leaks in fluid transportation and processing equipment is of high relevance in order to prevent harm to humans, nature and assets or just to prevent financial losses. Stationary installed in-situ sensors are used in plants to monitor high-risk areas on a sample base. An area-wide coverage of extended facilities is, however, a costly undertaking. Therefore, non-high-risk areas; that are still subject to possible leakages, are in general not monitored by gas sensors. In fact, routine inspections are commonly carried out using "smell, hearing, and eyesight". Formal inspections, particularly of pressurized equipment, are carried out during major revisions, e. g. each 3rd or 5th year using manually operated measurement equipment and manual data analysis.

This article provides an overview of the project RoboGas^{Inspector} (section 2). This targets the development of a human-machine system with autonomous mobile inspection robots equipped with remote sensing technology. The aim is to automate routine inspections for fluid leakages in plants and infrastructure. The use of remote sensing technology with mobile robots instead of in-situ (commonly semiconductor) gas sensors is a key differentiator to related work, see the overview in (Kowadlo and Russel 2008) and oil and gas specific work (Graf and Pfeiffer 2008, Persson and Anisi 2011). Details on research problems, principles and first experimental results for remote sensing of gas leakages and liquid spills using active spectroscopic (TDLAS) and passive infrared (IR) thermographic measurement systems are provided in sections 3, 4 and 5, respectively. The paper concludes with a summary and an outlook.

2. PROJECT OVERVIEW

A review of the state of the art and perspectives of robotic inspections of industrial sites (Kroll 2008) inspired the project RoboGas^{Inspector} (2011), which started in Dec. 2009. It is a joint research venture with four research, three industrial development and two application partners (a petroleum refinery and a gas transportation & distribution provider). The project consortium is led by the University of Kassel. The advantages of the planned system addresses

- Quality of process and results: improved inspection due to mobile remote gas sensing technology, central knowledge base increases locally available knowledge, increased coverage of extended inspection areas and increased inspection frequency with available staff

- Operator relief: easier inspection of remote areas by remote sensing technology, automation of repetitive, monotonous routine tasks, automated measurement evaluation and results documentation
- Profitability: more efficient and effective deployment of specialist staff, more time for human operators for activities that create higher value such as planning, supervision, and optimization, efficient deployment of sophisticated measurement devices

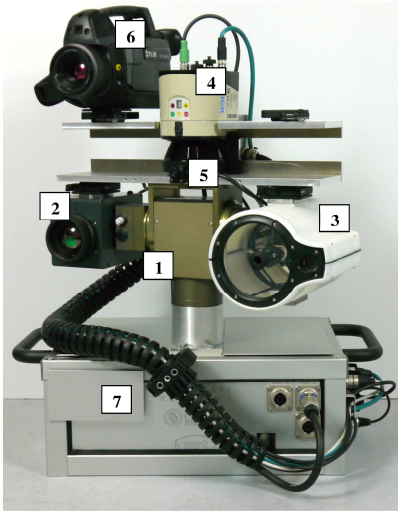

Fig. 1. Prototypic remote sensing head: A thermal camera (2), TDLAS device (3), laser scanner (4), video camera (5) and a thermographic camera for gas visualization are mounted on a pan-tilt unit (1). The computer and other electronics are housed in a control cabinet (7).

Fig. 2. Robot prototype with remote sensing technology.

The project activities have been grouped to the major working areas of 'Gas propagation and measurement', 'Mobile robots' and 'Human-robot-interaction'.

Gas propagation and gas measurement: To better understand the behavior of gas propagation from leaks, typical elementary leakage scenarios have been defined and are simulated using CFD (Computational Fluid Dynamics) tools. The simulations are validated with large scale outdoor gas dissemination experiments. The remote sensing is carried out by active and passive IR spectroscopic and thermographic technology. A prototypic sensor head has been designed and realized (Fig. 1). Measuring, processing and pattern recognition strategies as well as gas-detection/leak-localization algorithms have been developed.

Mobile robot platform: This working area covers the assembly of robot prototypes (see Fig. 2 for an impression of a prototype of the robotic system). Besides, mobility- related functions such as path and task planning for single-/multi-robot systems, autonomous path following, obstacle and collision avoidance are developed.

Human-robot Interaction: To increase the operator's acceptance of the overall system, the human is always in charge of supervisory control of the system. This means not only mission planning and supervision, but also user intervention if problems occur as well as enhanced human-robot interactions with the system (like using gesture control or augmented reality).

3. RESEARCH PROBLEMS AND APPROACH

The main research area for the authors is remote sensing of gas. With integral directional measurement devices (e.g. TDLAS in section 4) the problem is a) the detection of an abnormal gas concentration given varying background concentrations as well as varying path lengths and b) the localization of the leak source as a point in space and not as a direction. Ideas for possible strategies have been adopted from nature (bionics) as well as from engineering/statistics and have been extensively tested in simulations.

Thermal imaging devices on the other hand provide for an intensity matrix where the temperature disturbance due to a leak can be detected (see section 5) and also devices exist that can visualize the escaping gas (e.g. FLIR GF320). Here the questions are related to image processing, pattern recognition and machine learning. Also adding data from other sensors (e.g. depth or video) can provide helpful information and support the classification task. The algorithms are developed and tested in controlled lab environments and then transferred to testing in real industrial environments.

4. TDLAS: PRINCIPLE AND FIRST EXPERIMENTAL RESULTS

Optical remote gas measurement devices based on the tunable diode laser absorption spectroscopy (TDLAS) have, in contrast to classical in-situ gas sensors, the advantage that they don't need to enter a gas plume to make a concentration measurement. Cycle times of TDLAS measurement devices are shorter ($t_{In\text{-}Situ} \in [1, 90]$ s vs. $t_{TDLAS} \in [0.01; 0.1]$ s, (Bonow, Kroll 2011)), permitting to observe larger areas in a given period. The disadvantage however is that they provide for integral directional gas concentrations (typically in ppm·m: parts per million meter). Therefore, the position of a gas plume on the measurement path cannot be located from a single measurement.

4.1 Principle of measurement

Many technical gases like volatile hydrocarbons (e.g. Methane (CH_4) or Butane (C_4H_{10})) absorb radiation at different wavelengths in the IR spectrum. The absorption coefficient $\alpha(\lambda)$ is unique for every gas and can be used to identify the gas (finger print). If it is known, the average gas concentration $\overline{C}$ within the optical path length L can be determined by using the Lambert-Beer Law:

$$I_M(\lambda) = I_A(\lambda) \cdot \exp\left(-\int_0^L \alpha(\lambda) \cdot C(x) \cdot dx\right) = I_A(\lambda) \cdot \exp\left(-\alpha(\lambda) \cdot \overline{C} \cdot L\right) \quad (1)$$

whereas I_A is the measured light intensity without gas, I_M the measured light intensity with gas and $C(x)$ the local gas concentration at position x on the measurement path of the length L. Reassembling (1) provides for

$$\overline{C} = -\ln\left(I_M(\lambda) \cdot I_A(\lambda)^{-1}\right) \cdot \alpha(\lambda)^{-1} \cdot L^{-1}. \quad (2)$$

When using a remote gas sensor, L is in general unknown, and only the integral gas concentration $\tilde{C}$ can be determined:

$$\tilde{C} = L \cdot \overline{C} = -\ln\left(I_M(\lambda) \cdot I_A(\lambda)^{-1}\right) \cdot \alpha(\lambda)^{-1} \quad (3)$$

4.2 Remote gas measurement device RMLD

The RMLD emits an IR-laser beam and analyzes the light backscattered from any diffusely reflecting surface in the measurement path (e.g. walls, components, plants, (Frish et al. 2005)), thus $L = 2 \cdot L_R$ where L_R is the geometric path length of the measurement setup. The IR-laser diode of the RMLD can be tuned within a narrow spectral range. To determine the integral gas concentration, the laser is at first tuned to a reference wavelength λ_R, where methane has only a negligible influence on the measurement ($I_A(\lambda_R)$). For the second measurement, the laser is tuned to the wavelength of an absorption line of methane ($I_M(\lambda_{CH4})$). Based on these two measurements and assuming that the absorption characteristic of the atmospheric gases at the two wavelengths is constant or negligible ($\alpha_A(\lambda_R) \approx \alpha_A(\lambda_{CH4})$), the integral gas concentration can be calculated using (3).

As already mentioned, the RMLD can be used with most surfaces under different viewing angles. Own experiments have shown that most surfaces can be used up to a viewing angle of $|\varphi| \approx$ 70° (angle between surface normal and optical axis of the RMLD). Smooth or polished surfaces, e.g. made of metals like aluminum or stainless steel, that are observed normal to the surface (viewing angle of 0° to ≈5° and distance < 5 m), can reflect too much of the laser radiation and saturate the detector. In outdoor industrial environments, such surfaces are rare because most components (pipes, vents, flanges, etc.) are painted, coated or have a thin patina due to oxidation (rust).

Another problem occurs in case of measuring while the device is moving: The panning velocity $|\omega|$ has a direct influence on the minimal detectable gas concentration (Frish et al. 2007). This is because the RMLD averages the measured concentration in a time window of $t_M \approx$ 100 ms (update frequency of device is f_M = 10 Hz), thus the scanned volume at $|\omega| > 0°/s$ is larger than in the static case (note that the laser has a cone shape with an opening angle of $\varphi_{RMLD} \approx 1°$, so always a volume is measured). Conversely, the RMLD reports a smaller gas concentration if it is panned and the dimension of the plume orthogonal to the optical axis is smaller than the scanned volume. Fig. 3 shows the estimation of the minimal gas concentration within a ⌀ 90 mm cylinder (e.g. petri dish) that can be distinguished from natural methane in the atmosphere for different panning velocities and path lengths. In this test a gas concentration has been marked as distinguished if the RMLD readings exceed 130% of the background concentration. The results in Fig. 3 base on a mathematical sensor model with experimentally identified parameters.

Simple field tests and tests in the lab with the RMLD have shown that gas leaks with a mass flow of $\dot{m} \approx$ 2 mg/s (methane) can be distinguished from the natural methane concentration ($\overline{C}_A \approx$ 2-4 ppm) by an operator up to a path length of L_R=30 m (wind speed $v \approx$ 2-3 m/s orthogonal to the measurement path). The displayed values during the tests from the RMLD varied between $\tilde{C}(L_R = 30\,m)$ = 70-110 ppm·m and $\tilde{C}(L_R = 2\,m)$ = 220-320 ppm·m, where the measured average atmospheric methane was $\overline{C} \approx$ 2 ppm.

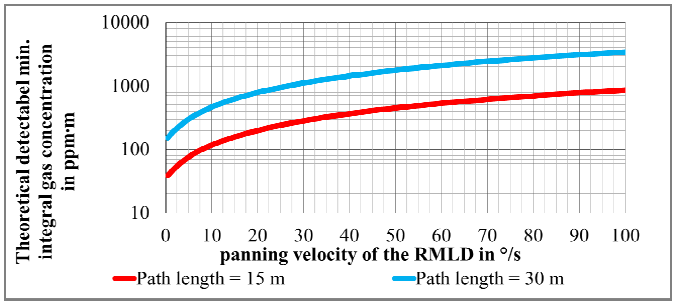

Fig. 3. Minimal methane concentrations in a ⌀ 90 mm cylinder dish that can be distinguished from the natural methane concentration (RMLD reading > 130% · $\tilde{C}_A$) of $\overline{C}_A$ = 2 ppm in the atmosphere for different measurement path lengths and panning velocities.

In this context, false alarms can arise if the alarm threshold used by the gas detection strategy is too low. On the contrary, with a high threshold, small leaks can be missed. This false/missed alarms are predominantly the result of the different path lengths and panning velocities of the sensor in combination with the measurement uncertainty of the RMLD (1σ = 3.7 ppm·m).

4.3 Using path length information for TDLAS-based measurements: First results

For robust automatic leak localization, it is necessary to determine the direction of the maximal gas concentration discernible from current location (Baetz et al., 2009). It is assumed that a gas leak is always located next to a surface. With the known position and orientation of the measurement device and path length to the maximum gas concentration, a potential leak position can be estimated. For this, a 2D laser scanner (Sick LMS 151) on a pan-tilt unit (Schunk PW90) is used to get 3D-depth information of the environment. These data can be used to calculate the average gas concentration for every RMLD measurement using (2).

Fig. 5 shows the result from a 3D depth scan of an outstretching utility corridor with depth information and Fig. 6 shows the measured integral methane in ppm·m produced

with a RMLD raster scan with reduced pan velocity ($|\omega|$ = 10°/s) of the area of interest. After the raster scan, the depth information of the 3D-depth scan is used to calculate the average gas concentrations (Fig. 7). In this step, the lateral shift between the optical axis of the measurement devices are taken into account.

Because of the considered path length and adapted panning velocity, the alarm threshold for the strategies can be reduced. Due to this approach, it is more likely to distinguish small gas leaks from atmospheric methane by using the path-length-independent average gas concentration than integral gas concentration.

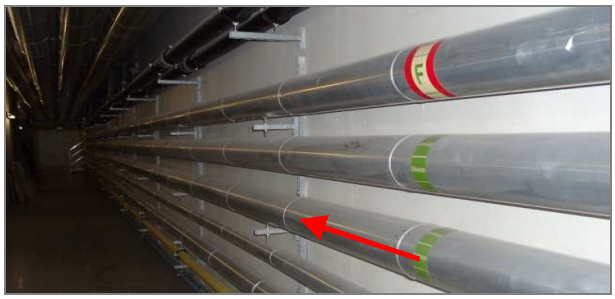

Fig. 4. Photography of an outstretched utility corridor.

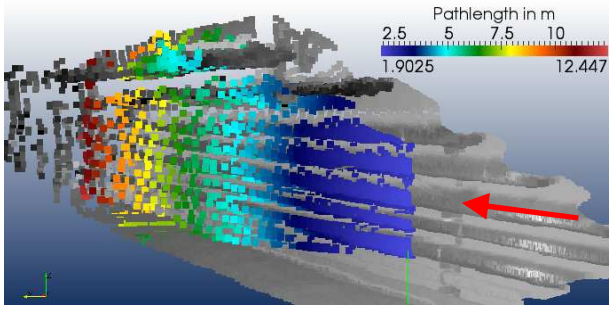

Fig. 5. Depth scan of the utility shaft from Fig. 4.

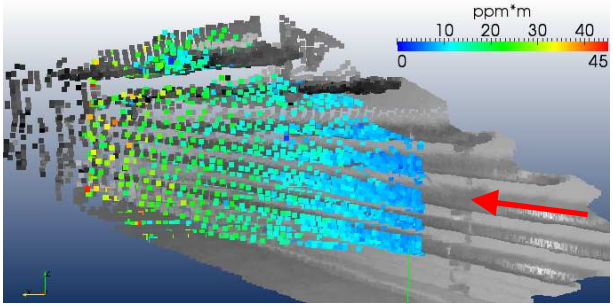

Fig. 6. Integral gas concentration measured from the viewpoint.

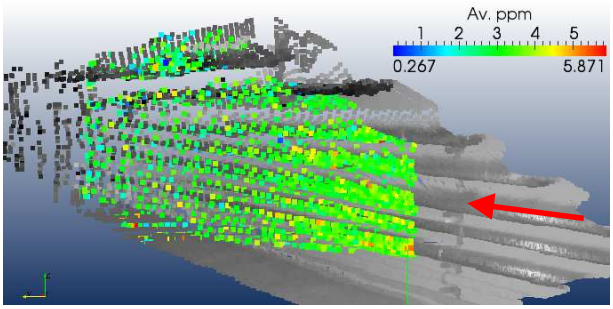

Fig. 7. Averaged gas concentration calculated from Fig. 6.

4.4 Discussion

By using the path length information, the RMLD measurements can be interpreted more easily than the integral gas concentration. In this context, the recommended fixed threshold strategy with a threshold of $\tilde{C}_A$ = 160 ppm·m (Frish et al, 2005) can theoretically be lowered to the maximal natural atmosphere methane concentration (≈ 4 ppm·L). However, due to the natural variation and due to the measurement uncertainties of the PTU angles, laser scanner readings and RMLD readings a higher value is to be expected. In addition, the search for the maximum gas concentration becomes easier, because variations in the measured concentrations due to a changing path length have now only a minor influence on the measurement. Up to now the compensation strategy has been tested under ideal laboratory conditions. A field test is planned to assess the robustness of the strategy. Moreover, the choice of a threshold for reliable automatic detection of small leaks under real world conditions has to be examined.

5. IR-THERMOGRAPHY: PRINCIPLES AND FIRST EXPERIMENTAL RESULTS

5.1 Basic principles and measurement effect

Every surface with a temperature above absolute zero (0 K) radiates energy. Its electromagnetic spectrum is in the IR-wavelength region from 1-100 µm. The spectral distribution of the ideal black body is given by Planck's law as the radiance per unit wavelength:

$$L_\lambda = \frac{2 \cdot h \cdot c^2}{\Omega_0 \cdot \lambda^5} \cdot \left[\exp\left(\frac{h \cdot c}{\lambda \cdot k \cdot T} \right) - 1 \right]^{-1}, \qquad (4)$$

with h: Planck's constant, c: speed of light in vacuum, λ: wavelength, Ω_0 : solid angle, and T: absolute temperature of the target surface. The total power radiated per unit area of a body for the entire spectrum is given by the Stefan-Boltzmann law as the radiant exitance:

$$M = \delta \cdot \varepsilon \cdot T^4 \qquad (5)$$

with δ: Stefan-Boltzmann constant, ε: emissivity (ε := 1 for black body target). With increasing object temperature, not only the total emitted energy changes, but also the maximum of the wavelength distribution shifts to shorter wavelengths. The position of the maximum of the distribution is given by Wien's displacement law:

$$\lambda_{\max} = b/T \qquad (6)$$

with Wien's displacement law constant b = 2898 mm·K. In processing plants, typical temperatures of pipes and vessels range from ambient temperature to 300 °C and therefore, the maximum of the radiation lies in the range of 5-10 µm.

Due to the absorption of mainly water and carbon dioxide, the atmosphere has a high transmission only for some IR-spectral regions, referred to as "atmospheric windows". The 8-14 µm window fits well for the targeted temperature range. Moreover, long wavelengths are less disturbed by the sun in

case of outdoor application. The used IR camera (Infratec VarioCAM® hr head) works in the 7.5-14 µm-spectral region.

At thermal equilibrium, the power of any incident radiation at the object's surface has to match the sum of absorbed, emitted and transmitted power. A black body target absorbs 100% of the incident radiation (i.e. $\alpha = 1$), a real body only a fraction ($\alpha_{real} < 1$). The emission coefficient ε of a real body is given as the ratio of absorption of the real body vs. the black body: $\varepsilon = \alpha_{real}$. A resulting problem for thermography is that a real body does not only radiate corresponding to its surface temperature, but reflects thermal radiation of surrounding heat sources. The sensor measures the totally emitted radiation. For instance, polished metals have emission coefficients in the range of $\varepsilon \approx 0.01 - 0.15$, meaning they specularly reflect thermal radiation of surrounding objects. Corroded or unfinished iron has $\varepsilon \approx 0.7$ and paint typically $\varepsilon \approx 0.95 - 0.99$, which is almost independent of color. Therefore, thermography is difficult to apply to uncolored, polished metal surfaces.

If gas escapes from a higher to a lower pressure reservoir without significant heat exchange with the environment, it expands, cools down and cooling the leaking object in the vicinity of the leak. Due to heat conduction, the temperature field disturbance propagates dependent on the thermal conductivity *k* of the material. Therefore the thermograpically sensed object temperature profile at the surface is disturbed by the leak. Metal conducts heat well (e. g. at 0 C: copper $k = 386$ W/(m·K), carbon steel with C = 0.5% $k = 55$ W/(m·K), stainless steel (V2A) $k = 16.3$ W/(m·K) (Maldague, 2001)). For this reason, the temperature field disturbance of leaking stainless steel pipes has spot type and is more extended for copper objects.

A liquid (e.g. water, petrol) with the surface exposed to the atmosphere will cause the liquid to vaporize without boiling. This phenomenon is called evaporation. The required energy causes cooling of the liquid or objects in the vicinity. Thermography can be used again to detect liquid spills on a surface based on the temperature profile.

5.2 Thermographic case study results

A measurement campaign has been designed and executed with pressured air leaks in pipes and instruments. A test stand was constructed to shield radiation from the environment (Fig. 8). Different pipes and instruments that vary in material, diameter, surface condition and leak type/size were tested under lab conditions. Pressured air was chosen because it is neither toxic nor explosive and easy to handle.

The measurements from the campaign clearly show a temperature drop around the leak area. For a leak diameter of 0.5 mm and a pressure drop of 5 bar, the cooling effect is around 0.5 K. Fig. 9 illustrates that the 'cold spot' varies with the material due to different heat conductivities and different surface conditions resulting from different emissivity.

The data were used to develop automatic pattern matching algorithms, which worked well in a lab environment. See Kroll et al. (2009) and Baetz et al. (2010) for further details.

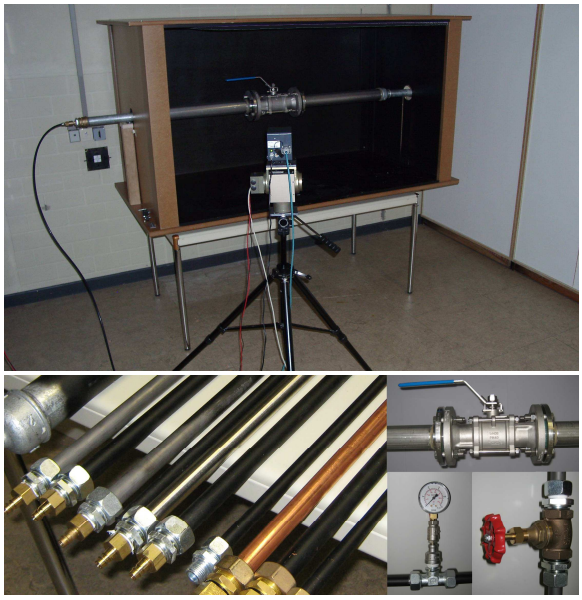

Fig. 8. Test stand for thermographic inspection (top), leaking pipes (bottom left) and instruments (bottom right).

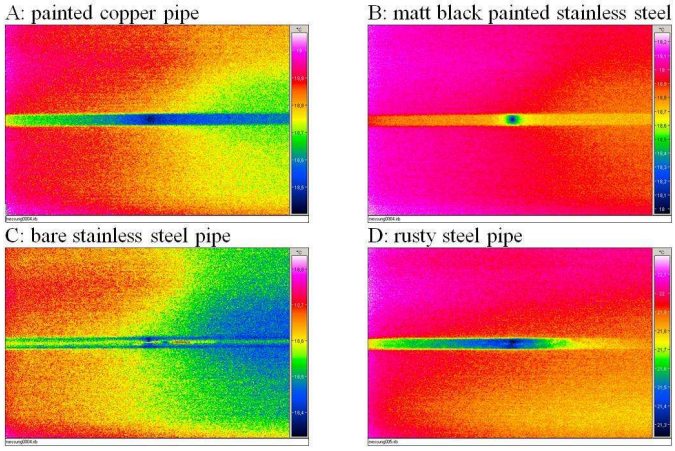

Fig. 9. Measurement results for different pipes with gas leaks. The false color code measurement spans of: A: 0.6 K, B: 1.2 K, C: 0.5 K, D: 0.9 K.

Fig. 10. Lab inspection robot with first-gen. sensor head.

For the detection of liquid spills, a simple case study was developed to test the feasibility. Water was poured on a basement floor 1 h before the measuring. The location was chosen to mimic a typical production environment. The sensors were mounted on a lab robot (Fig. 10) and measurements were taken with video and thermographic cameras. The water spill is not easy to detect in the video

image but stands out in the thermographic image (Fig 10). The temperature difference between spill and dry floor is 1.5 K. Fig. 10 also includes a gas leak in a pipe above the spill.

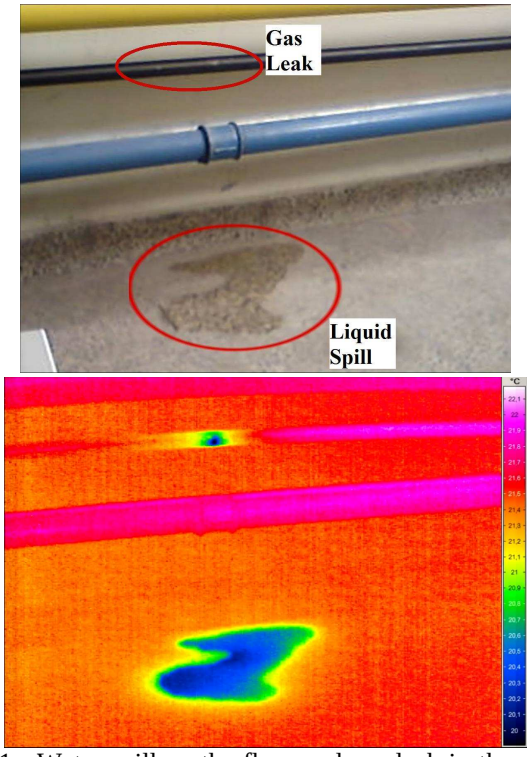

Fig. 11. Water spill on the floor and gas leak in the pipe in video image (top) and thermogram with temperature range from 20°C to 22.1°C (bottom).

5.3 Discussion

These first results on detection of small temperature effects ($\Delta T < 2$ K) look promising. However, Maldague (2001) states that in case of passive IR thermography $\Delta T = 1…2$ K is a first vague indication and $\Delta T > 4$ K a clear indication for an abnormality. Despite the technological advances (i.e. temperature resolution <0.03 K), it is assumed that these values are still valid for real-life unaided single-image thermography. The reason is that the condition of the target is unknown in general (unknown variations in emissivity vs. real variations in temperature). For this reason, the authors expect "straight" thermographic leak detection in an industrial setting to be challenges. Therefore, strategies that exploit further information (depth, color, multiple measurements) are investigated.

6. SUMMARY AND OUTLOOK

The mission for the project RoboGas[Inspector] is the simulation-based design and evaluation of a human-machine system with autonomous mobile inspection robots for remote IR-optical gas leakage detection and localization in plants. At the time of writing, the project is half-finished and preliminary results in the working area of remote fluid sensing are available.

Future work on the inspection module includes improvement of the detection and localization algorithms as well as data processing. A gas visualization camera will be added shortly. Tests in a gas compressor station and a petroleum refinery are scheduled to evaluate performance in an industrial setting.

ACKNOWLEDGMENT

The project RoboGas[Inspector] is funded by the Federal Ministry of Economics and Technology due to a resolution of the German Bundestag. The authors would like to thank the project partners and Dr. W. Baetz for valuable discussions and support.

REFERENCES

Baetz, W., Kroll, A. and Bonow, G. (2009). Mobile Robots with Active IR-Optical Sensing for Remote Gas Detection and Source Localization. *IEEE Int. Conf. on Robotics and Automation (ICRA 2009)*, Kobe, Japan, pp. 2773-2778.

Baetz, W., Kroll, A. and Soldan, S. (2010). On Gas Leak Detection of Pressurised Components by Using Thermograms and Pattern Recognition Algorithms. *8th Int. Conf. on NDE*, Berlin, Germany, pp. 503-512.

Bonow, G. and Kroll, A. (2011). Zur automatisierten Inspektion von Anlagen mittels Gasfernmesstechnik: Technologien und Geräte. *Proc. of* the *AUTOMATION 2011*, Baden-Baden, Germany, pp. 381-384.

Frish, M.B. et al. (2007). The next generation of TDLAS analyzers. *Society of Photo-Optical Instrumentation Engineers Optics East*, vol. 6765, pp. 76506-76517.

Frish, M.B. et al. (2005). *Extended Performance Handheld and Mobile Sensors for Remote Detection of Natural Gas Leaks - Phase II: Final Report*, [Online] http://www.netl.doe.gov/technologies/oil-gas/publications/td/ 41603_FinalReport.PDF, 11/2011.

Graf, B. and Pfeiffer, K. (2008). Mobile Robotics for Offshore Automation. *Proc. of the IART/EURON Workshop on Robotics for Risky Interventions and Environmental Surveillance. Benicassim, Spain.*

Kowadlo, G. and Russell, R.A. (2008) Robot odor localization: a taxonomy and survey. *Int. Journal of Robotics Research*, vol. 27, no. 8, pp. 869-894.

Kroll, A. (2008). A survey on mobile robots for industrial inspection. *Int. Conf. on Intelligent Autonomous Systems (IAS10)*, Baden-Baden, Germany, pp. 406-414.

Kroll, A., Baetz, W. and Peretzki, D. (2009). On Autonomous Detection of Pressured Air and Gas Leaks Using Passive IR-Thermography for Mobile Robot Application. *IEEE Int. Conf. on Robotics and Automation (ICRA 2009)*, Kobe, Japan, pp. 921-926.

Maldague, X.P.V. (2001). *Theory and Practice of Infrared Technology for Nondestructive Testing*. Wiley & Sons.

Persson, E. and Anisi, D. A. (2011). A Comparative study of robotic gas source localization algorithms in industrial environments. *IFAC World Congress*, Milano, Italy, pp. 899-904.

Skourup, C, and Pretlove, J. (2011). Remote inspection and intervention. *ABB Review*, no. 2, pp. 50-55.

RoboGas[Inspector]. (2011). *RoboGas[Inspector] - Project Website*. [Online] www.robogasinspector.de, 03/2012.

Vatland, S., Doyle P. and Andersen, T.M. (2007). Integrated operations: Creating the oil company of the future. *ABB Review*, no. 3, pp. 72-75.